Road Marking Detection Using LIDAR Reflective Intensity Data and its Application to Vehicle Localization

Alberto Hata[1] and Denis Wolf[1]

Abstract— A correct perception of road signalizations is required for autonomous cars to follow the traffic codes. Road marking is a signalization present on road surfaces and commonly used to inform the correct lane cars must keep. Cameras have been widely used for road marking detection, however they are sensible to environment illumination. Some LIDAR sensors return infrared reflective intensity information which is insensible to illumination condition. Existing road marking detectors that analyzes reflective intensity data focus only on lane markings and ignores other types of signalization. We propose a road marking detector based on Otsu thresholding method that make possible segment LIDAR point clouds into asphalt and road marking. The results show the possibility of detecting any road marking (crosswalks, continuous lines, dashed lines). The road marking detector has also been integrated with Monte Carlo localization method so that its performance could be validated. According to the results, adding road markings onto curb maps lead to a lateral localization error of 0.3119 m.

I. INTRODUCTION

A robust perception system is fundamental to autonomous cars safely navigate in urban environments. Road marking detection is a perception algorithm responsible for extracting horizontal signalizations like lane markings, crosswalks and stop signs from road surface [1]. The appropriate detection of road marking make possible keep the car in the correct lane and follow the local traffic codes. Localization is another problem of autonomous cars, particularly when covering urban places where obstacles as buildings and trees block the GPS satellite signal. To overcome this problem, maps have been used to estimate the vehicle localization. As road markings are common in the streets, they are usually employed as map features for localization in urban cities [2], [3].

Cameras have been widely used for road marking detection [1]. However, these sensors depend on external light conditions to perform this task. Generally, filters are necessary to handle shadows, excess and lack of light. This restriction can be suppressed by using infrared reflective intensity data returned by some LIDAR sensors. With intensity data it is possible to determine if a LIDAR beam intercepted asphalt or road painting independently of illumination condition.

Existing road marking detection methods that relies on LIDAR intensity data are focused on extracting only lane markings, thus they ignore other horizontal signalizations. The work of [4] analyses a point cloud with intensity data and checks for the highest intensity value. This value is used as threshold to segment the points into asphalt and lane

marking. Later, points pre-classified as lanes are projected onto a (x, y) plane where the y axis is towards to the road width. A 0.10 m window is slided in y direction to determine the regions with high gradient. These regions are classified as lane markings. [5] adopted a similar technique as previous one, but applied Hough transform after the gradient step for a better lane marking estimation. In [6] the asphalt intensity is obtained by computing the highest value of the intensity histogram. Then the point cloud is projected onto a binary colored map, with black for asphalt and white for lane marking candidates. Later, Canny filter was applied in the binary map for edge detection. A sliding window is passed through the resulting map and if the amount of white points in the window area were greater than a value it is classified as lane marking. In [3] is analyzed the intensity data obtained from a multilayer LIDAR and seeks for contiguous points that don't have considerable intensity variance. Those points are then placed on a grid map and then a Radon transform is used for line detection. [7] also uses a multilayer LIDAR, but includes an adaptive threshold to determine the ideal intensity value that best separates asphalt from road painting. The threshold is obtained by computing the intensity value that maximizes the variance in the intensity histogram. Then the UKF (Unscented Kalman Filter) is used to estimate lane parameters.

Differently, in the proposed method we can extract not only lanes, but any kind of road painting. For this we use a modified Otsu thresholding method to segment the point cloud returned from a Multilayer LIDAR (Velodyne HDL-32E) into asphalt and road marking. Basically, the Otsu method act like the adaptive threshold of [7] (obtains the intensity that maximizes the variance of the histogram), however we also analyze the separability measure and the histogram cumulative sum for higher accuracy. In addition, the idea of [3] is adopted to filter false positives. The previous methods also assume that the LIDAR intensity data is noisy free. So, we employed a LIDAR intensity data calibration algorithm proposed by [2] before the road marking detection.

For results validation we applied the proposed detector in a vehicle localization problem. In this way we compared the Monte Carlo Localization (MCL) performance using a map with curb data and another with both curb and road marking data.

This paper is structured as follows. Section II describes the road marking detector based on intensity data segmentation, Section III describes the localization method based on curb and road marking features, Section IV presents the experiments results and Section V concludes this works.

[1]Mobile Robotics Laboratory, University of São Paulo (USP), São Carlos, São Paulo, Brazil, {hata, denis}@icmc.usp.br
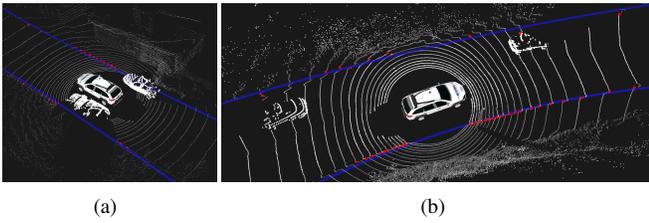
(a)   (b)

Fig. 1. Curb detection in urban streets with occluding obstacles in the sides.

II. ROAD MARKING DETECTION

Before detecting the road markings, first it is necessary determine the road boundaries in order to delimit the road marking search space. Thus, a curb detector is previously applied to estimate the road borders. For better results, the reflectivity intensity data returned from LIDAR sensor is calibrated in an offline step. Then, the road marking detection method based on Otsu thresholding is employed in the calibrated LIDAR data.

A. Curb Detection

As road markings only occur in road surfaces, we employed a curb detector to determine the road boundaries. The obtained road boundary is used to delimit the region that will be analyzed by road marking detector. The employed curb detector is an extension of obstacle detector proposed by [8]. Basically our curb detector analyses the compression level of consecutive rings returned by a multilayer LIDAR. As the compression is proportional to the obstacle slope, we can check if the compression value is inside a given threshold interval to detect curbs.

In order to determine this threshold interval, we first analyze the effect of LIDAR beams intercepting a flat surface. The radius of the formed rings are expressed by:

$$r_i = h \cot \theta_i, \qquad (1)$$

where r_i represents the radius of i-th ring and θ_i the corresponding beam angle and h the sensor height.

The distance between rings (ring compression) is calculated through consecutive radius difference:

$$\Delta r_i = r_{i+1} - r_i \qquad (2)$$
$$= h(\cot \theta_{i+1} - \cot \theta_i), \qquad (3)$$

where Δr_i is the distance between ring i and $i + 1$.

When a ring i intercepts an obstacle, the ring compression is changed to the interval:

$$\mathcal{I}_i = [\alpha \Delta r_i, \beta \Delta r_i(, \qquad (4)$$

where α and β are coefficients that determine the bounds of interval $\mathcal{I}$ constrained by $\beta > \alpha$.

Thus, we must determine α and β values that characterizes the curb obstacle.

In order to optimize this analysis, the ring data is stored in a circular grid. The grid is composed by i rows subdivided in j cells. In each cell $c_{i,j}$ is stored the average value of LIDAR

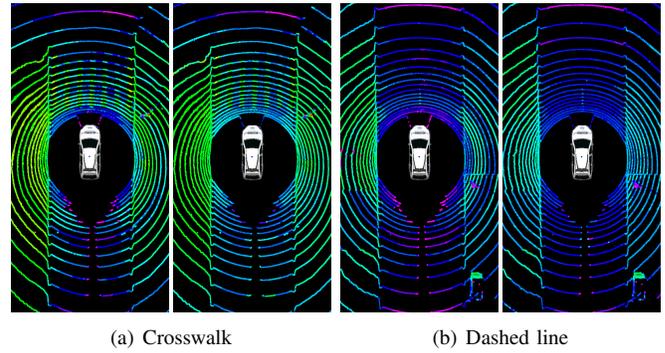(a) Crosswalk   (b) Dashed line

Fig. 2. Intensity calibration of two road markings. For (a) and (b), left is the original and right the calibrated intensity.

points position $(x_{i,j}, y_{i,j}, z_{i,j})$ and the range value $d_{i,j}$. Cells are pre-classified as curbs by checking the following criteria:

$$|d_{i+1,j} - d_{i,j}| \in \mathcal{I}_i. \qquad (5)$$

However, rely only on ring compression to detect curbs can lead to false-positives caused by objects with similar dimensions as curbs and occlusions. To enhance the detection, three filters are applied.

1) Differential Filter: As curbs are obstacles with height variation, a convolution mask is applied in each grid cell. The convolution operation determines the steepness of obstacles.

2) Distance Filter: Curbs are generally the closest obstacle to the vehicle. In this way only the closest cells to the vehicle are preserved.

3) Regression Filter: The result of distance filter can incorrectly preserve cells that are not curbs (e.g. another car traversing besides the vehicle). Thus, a robust regression method (least trimmed squares) is applied in the remaining cells.

After applying these filters the remaining cells are classified as curbs. The estimated left and right curb curves are then used to delimit the road area for road marking detection. Details of the curb detector are presented in [9]. Figure 1 illustrates the curb detection in urban streets and its robustness to occlusions.

B. LIDAR Intensity Calibration

Due to sensor manufacturer miscalibration, the returned intensity may not correspond to the expected values. For example, a LIDAR beam that intercepts the asphalt must return same intensity values in all road extent, but usually it doesn't occur. Consequently, the LIDAR intensity calibration is essential for correct detection of road markings.

In this work, we adopted the deterministic calibration method proposed by [2] which consists in the following steps:

1) Collect LIDAR points by traversing an arbitrary environment and associate them with pose data.

2) Place the LIDAR points onto a 2D grid. Each grid cell stores the list of points that fall in. For each point,

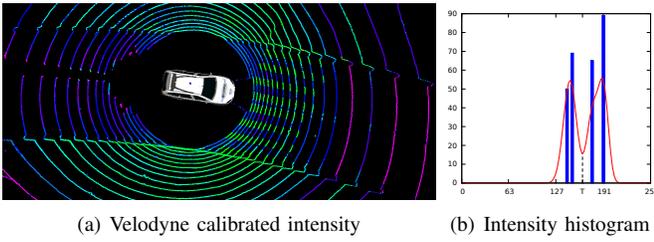(a) Velodyne calibrated intensity   (b) Intensity histogram

Fig. 3. Intensity histogram of a ring that intercepted a road marking.

only the intensity and the beam id information are maintained.

3) In order to compute the correct intensity value of a beam j that read an intensity a, we seek for all cells that contain the pair (j, a) in the grid. Then the average intensity is computed over these cells, but not taking in account the intensity whose beam is j. The calibrated intensity of (j, a) is the resulting average.

For each pair of beam id and intensity value, it is computed the calibrated return. If a certain intensity is not present in the grid, the calibrated return is computed by interpolating calibrated values with close intensities. The result of the calibration is a 32×256 table that comprehends in all combination of beam id and intensity values. So, for every LIDAR point, the intensity must be corrected by verifying the return value stored in the calibration table. Comparison of LIDAR intensity data before and after calibration is illustrated in Figure 2.

C. Otsu Road Marking Detection

For road marking detection we analyze the calibrated intensity of the LIDAR data. First, in order to restrict the analysis to the road area, we use the left $f_l(x)$ and right $f_r(x)$ curve models obtained from curb detector. The road surface is retrieved by extracting points inside the interval $f_l(x) < y < f_r(x)$.

Analyzing a LIDAR data returned from road surface (Figure 3(a)), the intensity value of points belonging to asphalt (≈ 190) and to road marking (≈ 127) are considerably distinct. The intensity histogram of these points presents a bimodal shape, with one mode grouping asphalt intensities and another grouping road marking intensities (Figure 3(b)). In this way, the Otsu thresholding [10] was applied to determine the intensity value T that maximizes the variance between background (asphalt) and foreground (road marking) classes. After applying the thresholding, the LIDAR points are segmented into asphalt and road marking.

In the following, steps of the road marking detector are listed:

1) Compute the normalized histogram of the intensity: Let n_i the i-th histogram value, M the number of road points, the normalized intensity (p_i) is computed by:

$$p_i = \frac{n_i}{M}.$$

2) Compute the cumulative sum: The cumulative sum $P(k)$ is the probability of a LIDAR ring point belong to a range $[0, k]$ and is calculated by:

$$P(k) = \sum_{i=0}^{k} p_i,$$

with $0 < P(k) < 255$ and L is the number of possible intensity values that the LIDAR represents.

3) Compute the cumulative mean: The cumulative mean $m(k)$ represents the mean intensity of the range $[0, k]$ which is computed by:

$$m(k) = \sum_{i=0}^{k} ip_i.$$

4) Compute the global cumulative mean: The global cumulative mean m_G is the mean intensity of whole histogram:

$$m_G = \sum_{i=0}^{L-1} ip_i.$$

5) Compute the global variance: The global variance σ_G^2 is the intensity variance sum over road points:

$$\sigma_G^2 = \sum_{i=0}^{L-1} (i - m_G)^2 p_i.$$

6) Compute the local variance: The local variance σ_L^2 is the variance of a specific intensity:

$$\sigma_L^2 = \frac{m_G P(k) - m(k)}{P(k)(1 - P(k))}.$$

7) Obtain the threshold: The threshold T is the value of k that maximizes σ_L^2:

$$T = \underset{0 \leq k \leq R-1}{\arg\max} \, \sigma_L^2(k).$$

8) Check the separability measure: The separability measure $\eta(T)$ represents the performance of using T to separate the histogram into two classes. Better separability is associated to $\eta(T)$ around 1. Thus we verify if $\eta(T)$ is greater than a given threshold t_η.

$$\eta(T) = \frac{\sigma_L^2(T)}{\sigma_G^2}.$$

9) Check the obtained separability intensity T: As the road marking intensity is associated with low values, T must be greater than a a certain intensity t_T.

10) Check the cumulative sum of $P(T)$: Roads generally have just a certain part of the asphalt covered by painting. Therefore, $P(T)$ must never be superior than a predefined threshold t_P.

11) Detect lane marking: If the point satisfy 8, 9 and 10 and the point with intensity is lower than T, classify the point as road marking.

The value T can be calculated once or recalculated for each new LIDAR data. Due to the variance of road marking and asphalt intensity along the streets (caused by wear), we recompute T when received a new LIDAR data.

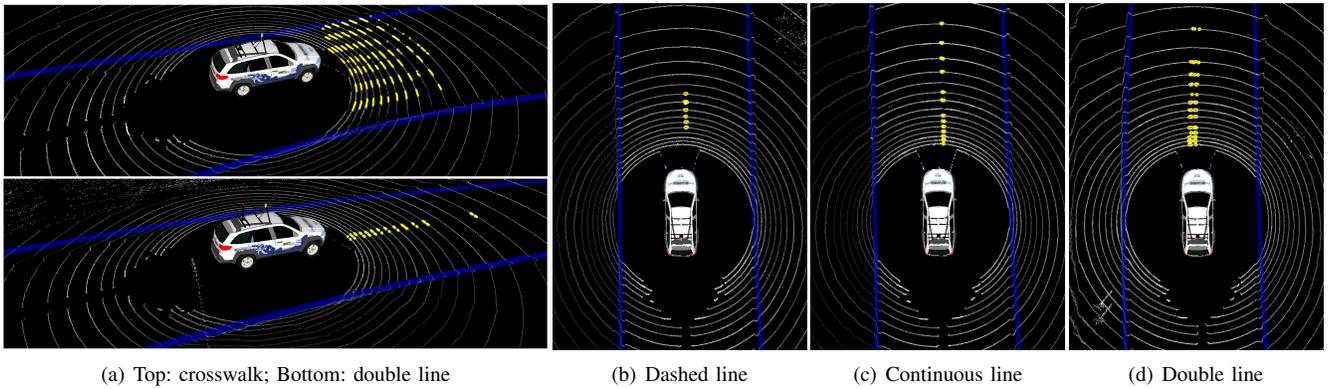(a) Top: crosswalk; Bottom: double line   (b) Dashed line   (c) Continuous line   (d) Double line

Fig. 4. Road marking detection through a modified version of Otsu method. Blue lines are the road bounds estimated by curb detector and yellow points correspond to the detected road marking.

(a) Intensity histogram   (b) Cumulative sum   (c) Cumulative mean   (d) Intensity variance
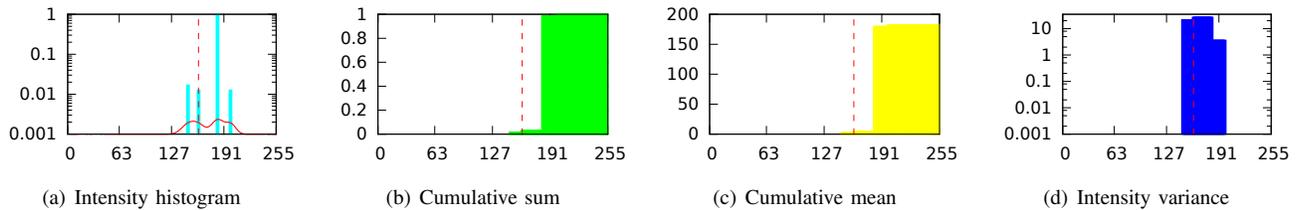
Fig. 5. Intensity histogram of Figure 4(b) of those points that are inside the curb bounds.

For better robustness, we discard the sequence of points detected as road marking which is longer than a certain length, as proposed by [3]. This is explained by the fact that road marking stripes don't have a long width (considering crosswalks and lane markings).

III. VEHICLE LOCALIZATION

In order to validate the road marking detector, it was applied in a vehicle localization problem. First, the point cloud formed by road markings and curbs were registered through Explicit Loop Closing Heuristic (ELCH) SLAM method [11]. Basically, ELCH aligns consecutive point clouds by minimizing the error in the loop closing point. The obtained map was placed into a binary grid map with 0.10 m resolution.

The Monte Carlo Localization (MCL) method was then used to localize the vehicle in the resulting map. In the MCL algorithm, initially a set of particles that represent the possible vehicle position are spread in the map (around the GPS position). Particles that best match curb and road marking with the map are preserved. The particle with the lowest error is chosen to represent the vehicle position.

IV. EXPERIMENTS AND RESULTS

Road marking detection experiments were performed through CaRINA 2 autonomous car prototype mounted with a Velodyne HDL-32E LIDAR sensor. The car odometry was obtained by Xsens MTi-G GPS device. First, we tested the road marking detector and then validated it in a vehicle localization problem. Thus, we compared the localization using only curb feature and using both curb and road marking features. The following subsections describe the conducted experiments.

A. Road Marking Detection

For road marking detection we assigned the threshold value $t_n = 0.90$ (maximum separability value), $t_T = 197$ (maximum intensity for road markings) and $t_P = 0.80$ (maximum cumulative sum). In Figure 4 is presented the road marking detection in urban streets. The blue line represents the road boundaries obtained from curb detector. These lines delimit the road markings search space. Yellow points represent the detected road marking by using the adapted Otsu method.

The intensity histogram aspect of the road represented in Figure 4(b) is shown in Figure 5. The Otsu method divided the bimodal histogram at $T = 160$ which resulted in the maximum variance of $\sigma_L^2 = 27.13$. At this point, the cumulative sum and mean indicate that the number of points start to increase at value T (i.e. the point that the asphalt intensity starts). The values of cumulative sum and separability measure were respectively $P(T) = 0.0128$ and $\eta(T) = 0.8589$ which satisfies t_P and t_n.

B. Road Marking as Localization Feature

The robustness of the detector was verified by using the road markings as a feature for map based localization. In order to build the environment map, the sequence of point clouds formed by curb and road marking were registered through ELCH offline SLAM method. We traveled a 822 m urban street and generated an occupancy map with 0.10 m resolution. Figure 6 illustrates the resulting map and the
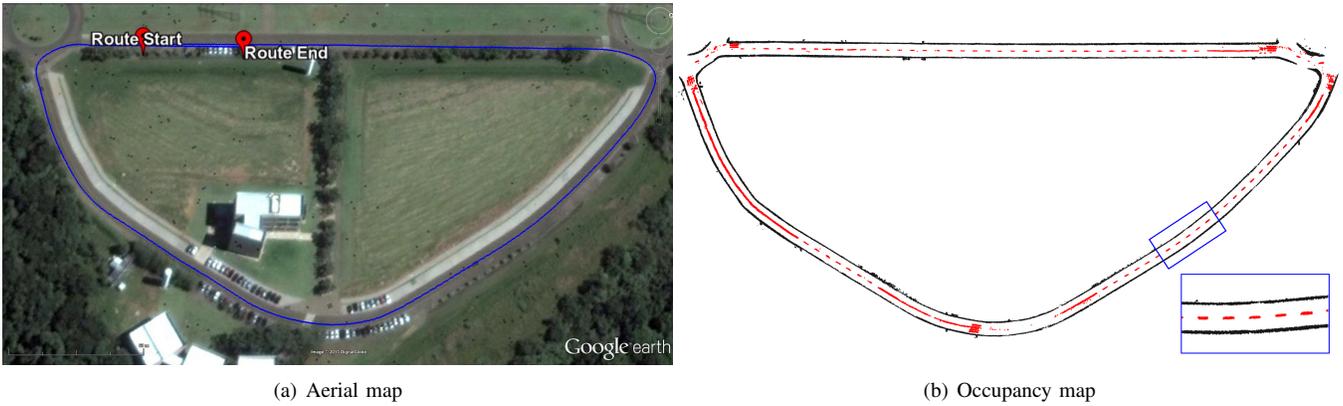
(a) Aerial map

(b) Occupancy map

Fig. 6. (a) Aerial map of the track used in the localization experiments. (b) Map of the same track formed by detected curbs (black dots) and road markings (red dots).

corresponding aerial map for comparison. As the map is most of part longitudinally symmetric, we mainly focused on the lateral localization.

For localization we adopted the MCL method configured to use at minimum 100 and at maximum 5000 particles, so the particle number is changed according to the localization error. These particles are initially distributed around the position given by the GPS device. Due to the GPS error it is necessary the vehicle run few meters for MCL convergence.

In the experiments we analyzed the MCL covariance error and the position error relative to ground truth. All experiment results were compared to MCL using only curb features (a map constituted only by curb points is used). The purpose of the comparison is to evidence that the use of road markings result in a better vehicle localization if used solely curbs. Table I presents the obtained covariance and position error values along the test track which confirms the performance improvement when adding road marking information. Regards to the lateral localization error, we observed a reduction of 53.56%, resulting in a average lateral error of 0.3119 m. The use of road marking also reduced the lateral and longitudinal covariance values in 71.34% (0.0542 m^2) and 59.69% (0.0391 m^2), respectively. As expected, in terms of longitudinal error it was observed a subtle reduction, resulting in a mean error of 1.1982 m.

Figure 7(a) and (c) illustrate graphically the position error along the test track if used only curb data and used both curb and road marking data, respectively. The circle radius size is proportional to the difference between the position returned by MCL and the ground truth. MCL covariance of the experiments are shown in Figure 7(b) and (d). A more detailed analysis of the localization error is presented in Figure 8. This graph shows the error value according to the traveled distance.

V. Conclusion

This paper presented a road marking detection that uses LIDAR reflective intensity data that is insensitive to light variation and can operate even without external illumination. The proposed road marking detector uses an adapted Otsu

thresholding algorithm which computes a value that optimizes the segmentation of point clouds into asphalt and road marking. In order to obtain better results, we also integrated the curb detector to delimit the road marking search area and the deterministic intensity calibration algorithm of [2]. Detection results showed the capacity of extracting different types of road markings (crosswalk, dashed line, continuous line).

We also applied the road marking detector to a vehicle localization algorithm for better performance analysis. First we registered a set of point clouds formed by curb and road marking data and then built an occupancy grid. In the localization experiment we tested the MCL algorithm with two configurations. In the first configuration we tested the localization using curb features, resulting in a 1.3174 m and 0.5823 m of longitudinal and lateral errors, respectively. Using curb and road marking features, we obtained 1.1982 m and 0.3119 m of longitudinal and lateral errors. In summary, using road markings together with curbs resulted in a lower

(a) MCL using Curb Data

	x (m)	y (m)	xy (m)	$\Sigma(x)$ (m^2)	$\Sigma(y)$ (m^2)
Mean	1.3174	0.5823	1.4947	0.1891	0.0970
Std. Dev	0.3931	0.4822	0.4068	0.5008	0.1304

(b) MCL using Curb and Road Marking Data

	x (m)	y (m)	xy (m)	$\Sigma(x)$ (m^2)	$\Sigma(y)$ (m^2)
Mean	1.1982	0.3119	1.2556	0.0542	0.0391
Std. Dev	0.2959	0.3363	0.2907	0.1045	0.0512

TABLE I

Statistics of MCL experiment. x, y and xy correspond to longitudinal, lateral and absolute Euclidean distance error, respectively. $\Sigma(x)$ and $\Sigma(y)$ correspond to MCL longitudinal and lateral error variances, respectively.
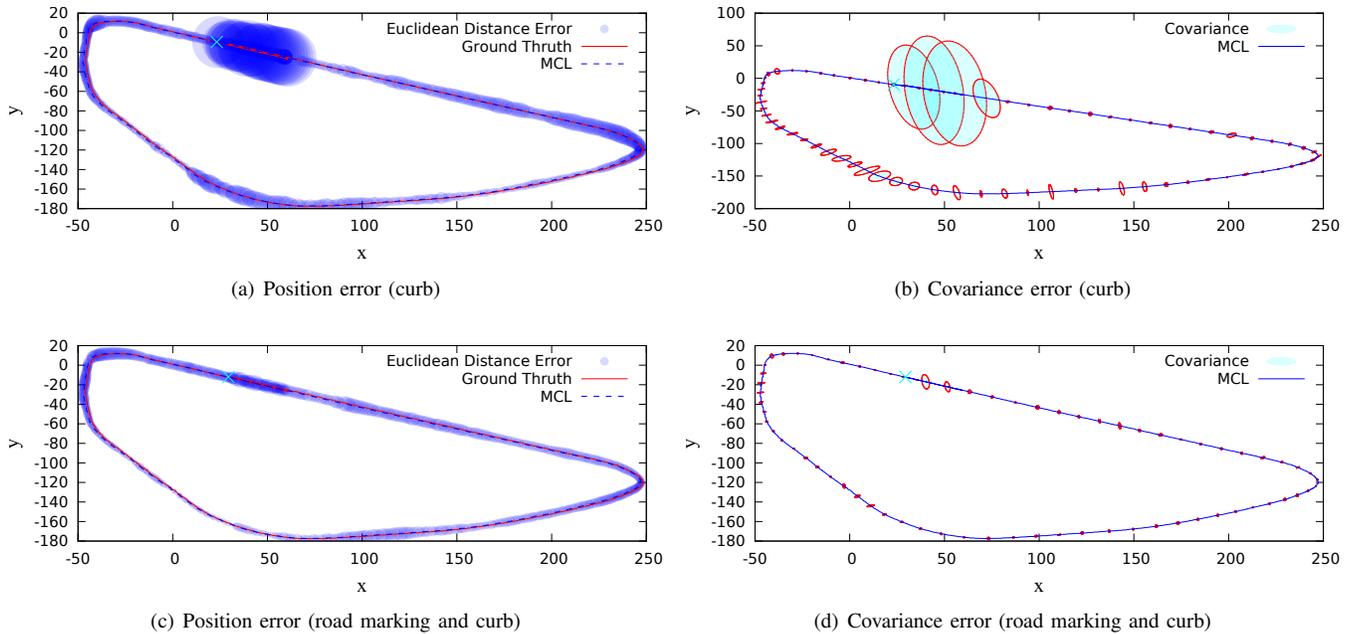
(a) Position error (curb)

(b) Covariance error (curb)

(c) Position error (road marking and curb)

(d) Covariance error (road marking and curb)

Fig. 7.   MCL covariance and position error. (a) and (b) are errors obtained when used only curb feature for localization. Ellipses x and y coordinates were shifted for better illustration. (c) and (d) are errors obtained when used road marking and curb features.

(a) Longitudinal error
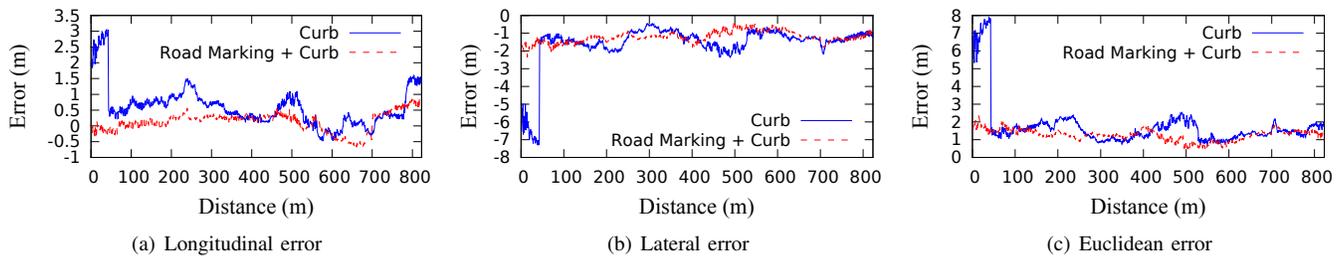

(b) Lateral error

(c) Euclidean error

Fig. 8.   Position estimation error along the trajectory. Blue line denotes MCL using curb feature and red line denotes MCL using road marking and curb features.

position error, lower covariance error and spent fewer iterations for convergence. The obtained localization errors were similar to other approaches, as [2], [3].

For next steps, we pretend classify the results of the road marking detector, in order to make the autonomous car traverse the streets according to the traffic codes.

ACKNOWLEDGEMENTS

REFERENCES

[1] A. Bar Hillel, R. Lerner, D. Levi, and G. Raz, "Recent progress in road and lane detection: a survey," *Machine Vision and Applications*, pp. 1–19, 2012.

[2] J. Levinson and S. Thrun, "Robust vehicle localization in urban environments using probabilistic maps," in *Robotics and Automation (ICRA), 2010 IEEE International Conference on*, may 2010, pp. 4372–4378.

[3] S. Kammel and B. Pitzer, "Lidar-based lane marker detection and mapping," in *IEEE Intelligent Vehicles Symposium*, Eindhoven, Netherlands, 2008.

[4] J. Kibbel, W. Justus, and K. Furstenberg, "Lane estimation and departure warning using multilayer laserscanner," in *Intelligent Transportation Systems, 2005. Proceedings. 2005 IEEE*, 2005, pp. 607–611.

[5] T. Ogawa and K. Takagi, "Lane recognition using on-vehicle lidar," in *Intelligent Vehicles Symposium, 2006 IEEE*, 2006, pp. 540–545.

[6] M. Thuy and F. Puente León, "Lane detection and tracking based on lidar data," *Metrology & Measurement Systems*, vol. XVII, no. 3, pp. 311–322, 2010.

[7] P. Lindner, E. Richter, G. Wanielik, K. Takagi, and A. Isogai, "Multichannel lidar processing for lane detection and estimation," in *Intelligent Transportation Systems, 2009.*, Oct 2009, pp. 1–6.

[8] M. Montemerlo and et al., "Junior: The stanford entry in the urban challenge," *Journal of Field Robotics*, vol. 25, no. 9, pp. 569–597, 2008.

[9] A. Hata, F. Osorio, and D. Wolf, "Robust curb detection and vehicle localization in urban environments," in *Intelligent Vehicles Symposium Proceedings, 2014 IEEE*, June 2014, pp. 1257–1262.

[10] N. Otsu, "A threshold selection method from gray-level histograms," *IEEE Transactions on Systems, Man and Cybernetics*, vol. 9, no. 1, pp. 62–66, Jan. 1979.

[11] J. Sprickerhof, A. Nüchter, K. Lingemann, and J. Hertzberg, "A heuristic loop closing technique for large-scale 6d slam," *AUTOMATIKA – Journal for Control, Measurement, Electronics, Computing and Communications*, vol. 52, no. 3, December 2011.